Analytic approach to modified effective-range theory for electron and positron elastic scattering

K. Fedus,[1,*] G. P. Karwasz,[1] and Z. Idziaszek[2]
[1]*Institute of Physics, Nicolaus Copernicus University, Grudziadzka 5/7, 87-100 Torun, Poland*
[2]*Faculty of Physics, Warsaw University, Hoża 16, 02-668 Warszawa, Poland*
(Received 6 May 2013; published 8 July 2013)

Modified effective-range theory (MERT) was developed in the 1960s to describe electron and positron scattering from atoms. The theory was frequently used to extrapolate measured total cross sections down to the zero-energy region, which is inaccessible experimentally. However, the applicability of the model was usually limited to the very low energy range where experimental data to be extrapolated are rare. We have proposed [Idziaszek and Karwasz, Phys. Rev. A **73**, 064701 (2006)] a different way of employing MERT by exploiting the properties of an analytical solution of the Schrödinger scattering equation with the long-range polarization potential. This alternative approach allows the validity of MERT to be extended to higher energies. At present we are applying this procedure for electron and positron scattering on He, H_2, Ar, and CH_4. The scattering amplitude and the effective-range parameters for s and p partial waves are obtained through a fitting inversion procedure applied to integral cross sections spanning most or all of the elastic region. The derived parameters are then used to obtain differential and momentum transfer cross sections; the agreement with experiments is very good.

DOI: 10.1103/PhysRevA.88.012704 PACS number(s): 34.80.Bm

I. INTRODUCTION

Renewed interest in electron scattering from atoms and molecules in the gas phase has been triggered by several factors. The imminent construction of industrial thermonuclear reactors requires modeling of low-temperature edge plasmas [1,2]. Cross sections for atomic targets such as H, He, Be, Li, and C and molecules such as H_2, BeH_2, and CH_4 should be determined. Secondly, a new roadmap in the semiconductor industries, requiring more precise plasma etching, aims to substitute CF_4 with more complex molecules, for which cross sections are still unknown. Thirdly, the interaction with electrons is also important in atmospheric environments—the policies for the reduction (and removal) of greenhouse pollutants require costly economic actions. Knowledge of cross sections in the low (and very low) energy region, hardly accessible experimentally, is a key factor in all these practical implementations.

Due to the complexity in describing short-range interaction potential, low-energy electron collisions are still the subject of intensive theoretical effort (see [3] and references therein). On the other hand, positrons, being twin particles to electrons but with positive charge, constitute an alternative probe of the same scattering problem [4,5]. Since no exchange interaction is present in positron scattering, they are easier to treat theoretically. The long-range polarization potential dominating at the limit of zero energy is attractive for both (i.e., electron and positron) projectiles while the short-range static potential is attractive for electrons and repulsive for positrons. As a result the positron cross sections at low (i.e., a few eV) collision energies are generally lower than those of electrons. Whereas in the very low region (below 1 eV) the opposite can happen—due to specific relations in the dominating s-wave phase shift, cross sections for positrons can be higher than for electrons. This is, in fact, the case of targets such as Ar, N_2, and H_2 [6]. Nevertheless, in analogy to electrons, an accurate theoretical analysis of positron scattering at very low energies is not an easy task since the interaction depends greatly on relatively small variations in the combined polarization-correlation potential [7].

Modified effective-range theory (MERT) for elastic electron and positron scattering from atoms and molecules was proposed a half century ago [8,9]. Due to its simplicity MERT has gained considerable popularity and has been frequently used to extrapolate measured cross sections to the very low energy range and very small scattering angles that are inaccessible experimentally [10–13]. In the standard approach the extrapolation relies on the effective-range expansion of scattering phase shifts of partial waves in powers of the projectile momentum k. An intrinsic drawback of such a procedure is the quick divergence of the k series with rising energy. Therefore, the applicability of the original MERT is limited to a very low energy range where the available cross-section data (to be extrapolated) are sparse. This limitation has been studied extensively by Buckman and Mitroy [14], who concluded that the theory is valid only below 1 eV in noble gases.

In [15] we proposed an alternative approach to the MERT series: Phase shifts were obtained solving analytically the Schrödinger equation with long-range polarization potential using Mathieu functions, and the effective-range expansion was introduced only for the short-range part of the interaction potential. In [15] we analyzed particularly the experimental positron-scattering total cross sections for Ar and N_2 up to 1 eV. Successively, in [16] we tested the new MERT approach for electron scattering from N_2 up to an energy of about 10 eV, showing that even in so-called shape resonances a dominant role can be attributed to the long-range polarization potential.

In the present paper we perform a more extensive MERT analysis of electron and positron scattering from light atomic and molecular targets: He, H_2, Ar, and CH_4, using different sets of recent experimental total cross sections (TCS). The two latter targets show a Ramsauer-Townsend (R-T) minimum for electrons [17,18]. For positrons, all four targets show a

*kamil@fizyka.umk.pl

rise of TCS in the zero-energy limit. The search for the R-T minimum in positron scattering was formulated in previous experiments [19]. Here we perform a systematic analysis of this problem.

To validate our approach the parameters of the scattering potential (scattering lengths and effective ranges for single partial waves: s, p, and d for heavier targets) derived from different experimental sets of integral elastic cross sections (obtained from TCS by subtracting inelastic channels) are further used to calculate elastic differential cross sections (DCS) and momentum transfer cross sections (MTCS) using a wide experimental database.

The paper is organized as follows: In Sec. II we describe briefly the principles of modified effective-range theory. In particular, we compare the standard versions of MERT with the latest approach [15]. Section III describes the choice of experimental data used for fitting procedures and comparisons. Section IV is devoted to MERT analysis of electron and positron scattering from selected targets. The main conclusions are summarized in Sec. V, including advantages and limitations of current MERT analysis. Finally, two appendixes give more details about MERT.

II. MODIFIED EFFECTIVE-RANGE THEORY

Effective-range theory (ERT) was developed primarily to calculate phase shifts of the wave function in nuclear scattering [20,21]. Later it was adapted to electron and positron scattering from atoms that are dominated by long-range isotropic polarization force at very low energies. Since the original energy expansion of scattering phase shifts given by ERT breaks down for long-range potential, O'Malley *et al.* [8,9] introduced an extended approach called modified effective-range theory (MERT). Since that time MERT has been widely used by experimentalists to extrapolate the zero-energy cross sections and/or to compare beam- and swarm-derived electron-scattering data in noble gases [22–30] and highly symmetric molecules such as CH_4 [10,31] and CF_4 [12].

In typical MERT analysis, the partial-wave scattering phase shifts are expressed as a series of the projectile (electron or positron) momentum k containing few adjustable parameters. In the basic version, so-called MERT4, there are four fitting parameters and the phase shifts related to particular partial waves are given as [32]

$$\tan\eta_0(k) = -Ak\left[1 + \frac{4}{3}\alpha k^2 \ln(k)\right] - \frac{\pi}{3}\alpha k^2 + Dk^3 + Fk^4, \tag{1}$$

$$\tan\eta_1(k) = \frac{\pi}{15}\alpha k^2 - A_1 k^3, \tag{2}$$

$$\tan\eta_l(k) \approx \frac{\pi\alpha k^2}{8(l-1/2)(l+1/2)(l+3/2)}, \quad \text{for } l > 1, \tag{3}$$

where l is the angular momentum quantum number, α is the dipole polarizability of the target, A is the s-wave scattering length, and D, F, and A_1 are additional fitting parameters. Here Eq. (3) is exact at the low-energy limit [8], and this result can be also reproduced using a first-order Born approximation.

The total cross sections (TCS) and momentum transfer cross sections (MTCS) are given by the partial-wave expansions as

$$\sigma_t = \frac{4\pi}{k^2}\sum_{l=0}^{\infty}(2l+1)\sin^2\eta_l(k), \tag{4}$$

$$\sigma_m = \frac{4\pi}{k^2}\sum_{l=0}^{\infty}(l+1)\sin^2[\eta_l(k) - \eta_{l+1}(k)], \tag{5}$$

while the differential cross sections (DCS) can be calculated from

$$\frac{d\sigma}{d\omega} = \frac{1}{k^2}\left|\sum_{l=0}^{\infty}(2l+1)\exp(i\eta_l)\sin(\eta_l)\mathrm{P}_l(\cos\theta)\right|^2, \tag{6}$$

where $\mathrm{P}_l(x)$ are the Legendre polynomials and θ is the scattering angle.

Ali and Fraser [33] introduced higher-order terms in expansions of p-wave ($l = 1$) and d-wave ($l = 2$) phase shifts resulting from short-range components of polarizability. Using these results Buckman and Mitroy [14] introduced MERT5 and MERT6 with five and six fitting parameters, respectively. This allows the applicability of MERT to be extended to higher energies, although still below 1 eV.

In order to extend the valid energy region to represent the s-wave ($l = 0$) phase shift, O'Malley and Crompton [24] proposed to add another parameter in Eq. (1)—see Eq. (A8) in Appendix A. Recently, Kurokawa [29] and Kitajima [30] showed that only when using the s-wave phase shift in this modified form was it possible to fit MERT reasonably well up to 1 eV with all their recent experimental cross-section data for noble gases. Extended MERT versions with five, six, and seven fitting parameters are described in detail in Appendix A.

The present authors develop an alternative way of employing MERT [15]. The Schrödinger equation with long-range polarization potential (r^{-4}) was solved in an analytical way using Mathieu functions, while the effective-range expansion was introduced exclusively for the short-range potential. Accordingly, using the Mathieu functions one can find the following analytical expression for the scattering phase shift of each partial wave [8]:

$$\tan\eta_l = \frac{m^2 - \tan^2\delta_l + \tilde{B}_l\tan\delta_l(m^2-1)}{\tan\delta_l(1-m^2) + \tilde{B}_l(1-m^2\tan^2\delta_l)}, \tag{7}$$

where $\delta_l = \pi(\nu - l - 1/2)/2$, and m and ν are energy-dependent parameters which have to be determined numerically from analytical properties of Mathieu functions. We have already described this procedure in detail in Refs. [15,16]. Nevertheless for self-consistency of this paper we recall it briefly in Appendix B.

The contribution of short-range interaction is hidden in the parameter $\tilde{B}_l(k)$ related to the phase shift induced by the short-range potential [15,16]. This parameter is expanded around zero energy for each partial wave separately: $\tilde{B}_l(k) \approx B_l(0) + R_l R^* k^2/2 + \cdots$, where R_l can be interpreted as the effective range for a given partial wave. Here $R^* = \sqrt{\alpha e^2\mu/\hbar^2}$ denotes a typical length scale related to the r^{-4} interaction, where e is the elementary charge, μ is the reduced mass of the projectile/target system, and $\hbar$ is the Planck constant. In the particular case of $l = 0$, $B_0(0)$ can be expressed in terms of s-wave scattering length as $B_0 = -R^*/A$.

The number of partial waves necessary to be treated by Eq. (7) can be estimated by comparing the energy of the projectile with the height of the centrifugal barrier $E_b(l) = 1/4E^*l^2(l+1)^2$ for the r^{-4} interaction [34], where $E^* = \hbar^2/2\mu R^{*2}$ is the effective energy. The particle can penetrate the inner (short-range) part of the potential only when $E > E_b(l)$. In most cases, the elastic TCS can be described considering only the contribution of s- and p-wave phase shifts and sometimes, for heavier targets, also the d-wave phase shift. The small contributions related to the higher partial waves are described using an approximation by Eq. (3).

III. CHOICE OF EXPERIMENTAL DATA

As an experimental database we use total cross sections (TCS) that can be measured in an absolute way. Differential cross sections (DCS) bring much more information but they need normalization procedures, while momentum transfer cross sections (MTCS) require more fitting parameters. TCS extending in recent electron and positron experiments [29,35–37] well below 1 eV should therefore assure better certainty on the MERT results. As far as electron scattering is concerned, rather good agreement on TCS has been obtained (see [17,18]). In this paper we will limit the analysis of electron scattering to three beam experiments extending to the lowest energies: time-of-flight data from Bielefeld [10,11] and Canberra [26] as well as the photoelectron-based data by the Tokyo group [29] extending down to 60 meV.

Positron experiments are much more tedious and they use a variety of methods to obtain a sufficient signal-to-noise ratio. The early experiments from Wayne State University (Detroit) [19] were based on a long (109 cm), curved scattering cell and a weak guiding magnetic field. The energy resolution of that machine was good (probably 0.1–0.2 eV) and the angular resolution was moderate (better than 10°–20°). As shown by the group from Canberra [38] for Ar, the Detroit data can be qualitatively brought into agreement at the low-energy limit with their recent data [36] if a correction by some +20% for the angular resolution is made. The recently developed Canberra positron apparatus [36] uses a strong magnetic field (500 G) so the cross sections have to be deconvoluted, extrapolating the measured signal to the zero field. Another early setup, from Tokyo Yamaguchi University [39], used a weak magnetic field (3.6–27 G), 7-cm-long scattering cell but wide (6–9 mm diameter) entrance and exit apertures. As a consequence, the measured cross sections were underestimated at their low-energy limit. However, as we showed in detailed analysis for benzene and N_2, the Tokyo data can be brought into good agreement with recent experiments [40] if a correction for the angular resolution is performed. The original apparatus developed at Trento University [41] used a scattering cell length (10 cm) similar to Suoeka's but much narrower (1.5 mm diameter) apertures; the guiding field was about 9 G. As we showed for N_2 and benzene, the possible angular resolution corrections are below 1% in the whole (0.4–20 eV) energy range. More recently a modified configuration of the Trento apparatus [42] was introduced. It uses a very short (2.4 cm) scattering cell and probably a low counting rate (in the order of 1 e^+/s). As pointed out by Mitroy and co-workers [43], the results of Zecca *et al.* [42] for H_2 from this recent experimental configuration disagree with other measurements and theories.

IV. MERT ANALYSIS OF ELECTRON AND POSITRON CROSS SECTION

A. Helium

Helium is considered a benchmark in electron scattering as the agreement between experiments and theories is generally very good. However, there are still only a few experimental TCS data sets available below 1 eV; see [17]. The low dipole polarizability $\alpha = 1.407a_0^3$ [44] provides relatively high effective energy $E^* = 9.671$ eV. Therefore, the d wave ($l = 2$) needs an energy of at least $E_b(2) \approx 87$ eV to overcome the repulsion of the centrifugal barrier. Thus, two partial waves, s and p, should be sufficient to explain TCS in the whole energy range for elastic scattering of electrons, $E < 20$ eV (below the first electronic excitation), and positrons, $E < 15$ eV (below the positronium formation threshold).

The experimental results of Buckman and Lohmann [26] were chosen as the electron input TCS data to be extrapolated. The fitting results using an unweighted least-squares method are shown in Fig. 1(a). The corresponding parameters of the effective-range expansion are given in Table I. It can be seen clearly that the present MERT is able to reproduce TCS in the whole elastic scattering region. The overwhelming contribution comes from the s wave, and the derived scattering length $A = -R^*/B_0 \approx 1.186a_0$ stays in perfect agreement with the other experimental and theoretical results; see [17] and references therein. Note that the scattering length A is numerically equal here to the value of R^*, the characteristic distance of the r^{-4} interaction. Since the contribution of the effective-range correction (R_1) in the p wave is rather small, one cannot fully rely on results for this parameter derived from the fitting procedure. Nevertheless, using the parameters given in Table I, one can calculate the momentum transfer cross section (MTCS), shown in the inset of Fig. 1(a), staying in pretty good agreement with experimental data. The maximum discrepancy with the results of Ref. [45] is less than 4%.

Furthermore, the calculated scattering s-wave and p-wave phase shifts (η_0 and η_1) have been used to determine differential cross sections (DCS). The comparison of these calculations with experimental data [46–49] is shown in Figs. 1(b)–1(d). Two solely partial waves reproduce the experimental DCS very well at 5 eV. At 20 eV, in order to get a reasonable agreement, we take into account additionally the contribution of 100 higher partial waves ($l > 1$) using the approximation by Eq. (3). However, at 12 eV the addition of higher partial wave phase shifts does not improve the agreement with the experiment. Probably, in an intermediate energy range of elastic scattering (10–12 eV), the explicit inclusion of the d-wave exact phase shift would be needed. Maybe some shape resonance can play a role at this energy domain. However, it proves to be difficult to find the d-wave phase shift when using TCS data solely: The contribution from d wave to TCS is negligible and its numerically obtained value is unstable.

Positron-scattering cross sections from helium are much more fuzzy. All four sets of data [35,50–52] available below 1 eV indicate a rise in the total cross sections towards zero

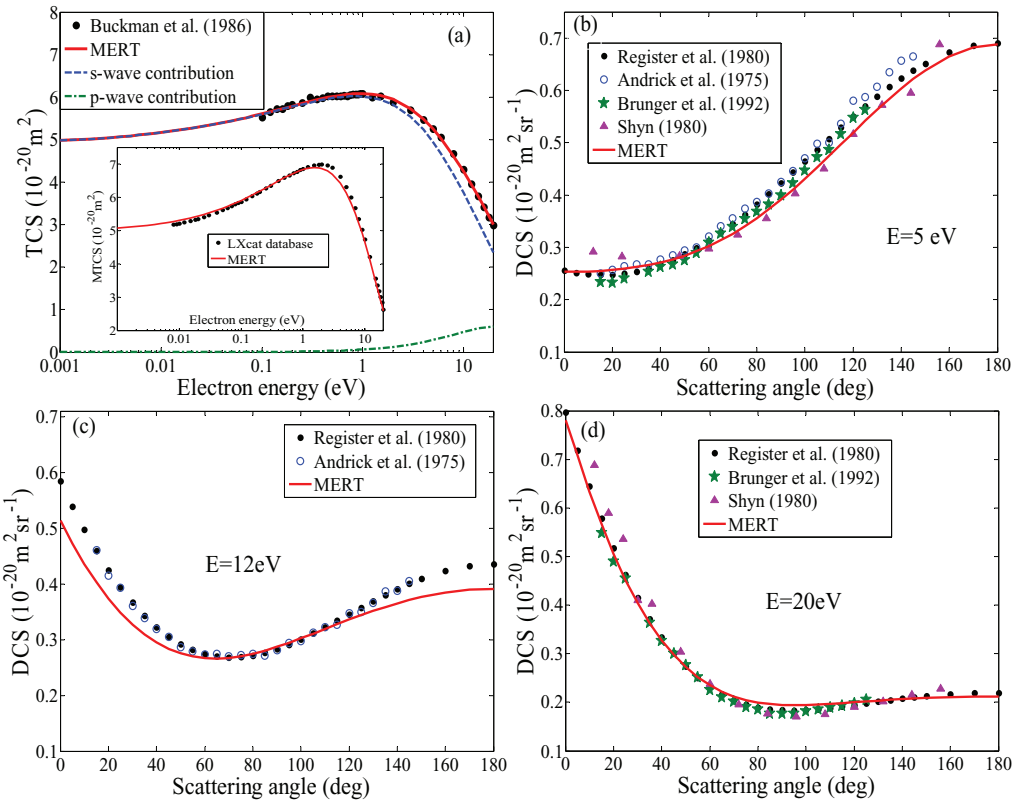

FIG. 1. (Color online) MERT analysis for electron scattering from helium: (a) total cross section versus energy. Experimental data (dots) are from Ref. [26]. The inset shows MERT calculations of momentum transfer cross section compared with experimental data from Ref. [45]. (b)–(d) Differential cross section versus scattering angle at 5, 12, and 20 eV, respectively. Experimental data are from Refs. [46] (open circles), [47] (filled dots), [48] triangles, and [49] (stars).

energy but they differ in absolute values by up to a factor of 4. In Fig. 2(a) we compare MERT fits using two partial waves to the most recent data of Sullivan *et al.* [52] and Karwasz *et al.* [35] (the resonant structure present in the latter data has been omitted for the purpose of fit). The fitting has been performed up to a projectile energy of 15 eV. The fitting parameters are given in Table I. In particular, the scattering lengths are $-0.45a_0$ and $-0.59a_0$, for the data of Sullivan *et al.* and Karwasz *et al.*, respectively. These values are in reasonably good agreement with results predicted by other approaches, varying from $-0.47a_0$ to $-0.57a_0$ (for example, see [53,54]). The other three parameters, B_1, R_0, and R_1, are significantly different for the two experimental data sets although they keep the same sign.

TABLE I. Parameters of the effective-range expansion for electron and positron scattering from helium: $A = -R^*/B_0$ (scattering length), B_1 (zero-energy contribution for p-wave), R_0 (s-wave effective range), and R_1 (p-wave effective range). The characteristic distance is $R^* = 1.186a_0$ and the characteristic energy is $E^* = 9.671$ eV.

	A (units of a_0)	B_1	R_0 (units of a_0)	R_1 (units of a_0)
e^--He Ref. [26]	1.186	−20	0.01	−100
e^+-He Ref. [35]	−0.59	−1.29	−0.28	1.16
e^+-He Ref. [52]	−0.45	−0.71	−1.45	0.29

Even if the two considered TCS sets are different, both of them indicate the existence of the R-T minimum: The s-wave phase shift (η_0) goes through zero at about 2–3 eV, as shown in Fig. 2(b). Moreover, η_0 stays in reasonably good agreement with the results of the stochastic variational method of Zhang and Mitroy [54] and the *ab initio* calculations of Van Reeth and Humberston [55]. Furthermore, we show that the d-wave phase shift of the latter work can be well reproduced using the approximation by Eq. (3). It is evident from Fig. 2(b) that the important difference between the MERT and *ab initio* results appears only for the p-wave phase shifts at higher energies, $E > 2$ eV.

B. Argon

Argon is a target with a higher polarizability ($\alpha = 11.23a_0^3$ [44]) than helium and thus is characterized by much lower effective energy $E^* = 1.212$ eV. Consequently, the d wave needs only $E_b(2) \approx 10.9$ eV to overcome the repulsion of the centrifugal barrier. This value is comparable with the ionization potential of argon (15.8 eV). Therefore, the contribution of the d wave can play an important role at higher energies of the elastic scattering region. Indeed, we have checked that at least three partial waves are needed in order to reproduce experimental TCS for electrons up to 10 eV.

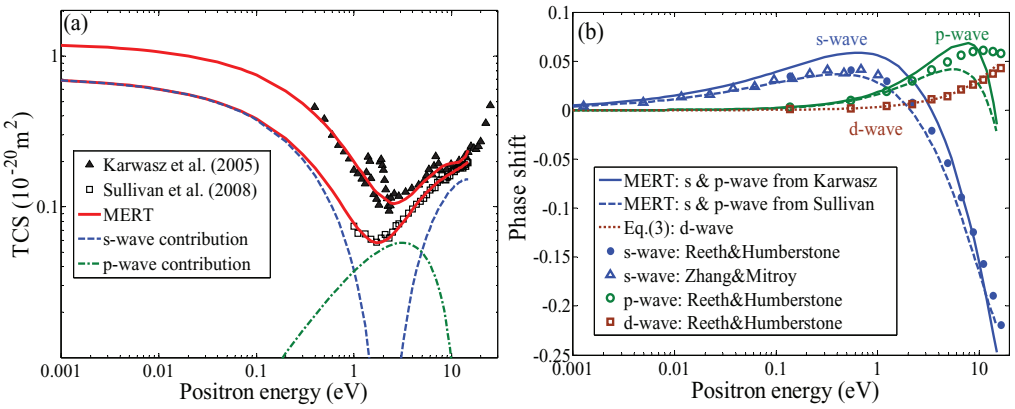

FIG. 2. (Color online) MERT analysis for positron scattering from helium: (a) total cross section versus energy. Experimental data are from Ref. [35] (triangles) and Ref. [52] (squares). The s- and p-wave contributions are shown only for data of Ref. [52]. (b) The scattering phase shifts versus energy. Solid lines and dashed lines are MERT calculations for s-wave and p-wave phase shifts based on TCS data of Refs. [35] and [52], respectively. Additionally, the dotted line represents the d-wave phase shift estimate obtained from Eq. (3). Present calculations are compared with theoretical results of Zhang and Mitroy [54] and Van Reeth and Humberston [55].

In Fig. 3(a) we show that the MERT fits to the data measured by Ferch *et al.* [11], Buckman and Lohmann [26], and Kurokawa *et al.* [29]. Some discrepancies are visible only in the region of the R-T minimum if compared to data by Buckman and Lohmann and in the region 0.1–0.3 eV using data by Kurokawa *et al.* The corresponding parameters of the effective-range expansion are given in Table II. All obtained values are quite close for these three sets except for the s wave of data by Kurokawa *et al.* It stays somehow in agreement with the work of Kurokawa *et al.* [29], who analyzed their data using the standard version of MERT. They could obtain good agreement only when using a modified (empirically found) equation for the s-wave phase shift [see Eq. (A8) in Appendix A] proposed by O'Malley and Crompton [24]. The derived scattering lengths A, namely $-1.5a_0$ for Ferch *et al.* and Buckman and Lohmann, and lower, $-1.4a_0$ for Kurokawa *et al.*, are in good agreement with results available in the literature. The latter varies in the range from $-1.46a_0$ to $-1.63a_0$, according to different determinations—theoretical, beam, and swarm experiments [17].

In the further analysis MTCS and DCS were calculated. For the purposes of this study the scattering phase shifts obtained from the TCS of Ferch *et al.* were used, but also the data of Buckman and Lohmann assure similarly good results. In addition to MERT-derived η_0, η_1, and η_2, we used 100 higher partial waves, the contributions of which were estimated using Eq. (3). Figure 3(b) presents calculated MTCS compared with the swarm-derived data of Milloy *et al.* [56] and Haddad and O'Malley [57]. In general the agreement has to be judged as good except for the region of the R-T minimum, where the present theoretical depth is shallower by about 20%. Furthermore, in Fig. 3(c) we compare MERT calculations of DCS with the low-energy data of Weyhreter *et al.* [58]. To the best of our knowledge, these data are as yet the only available experimental DCS measured in the region of R-T minimum. In addition, an example of MERT calculations at higher energy, $E = 5$ eV, compared with experiments [59–62] is shown in Fig. 3(d). From the obtained results it is clear that the current MERT reproduces experimental data sets very well despite significant variations of DCS over the considered energy range.

For positron scattering the three recent sets of data, from Karwasz *et al.* [6], Jones *et al.* [36], and Zecca *et al.* [63], have been used for MERT analysis. In Fig. 4(a) we show the fits performed up to 5 eV, below the positronium formation threshold. In this range of energy only two partial waves are sufficient to find reasonably good agreement with all experimental data sets. The obtained parameters of the effective-range expansion are given in Table II. In particular, the s-wave scattering lengths are $-5.52a_0$, $-4.11a_0$, and $-4.66a_0$, respectively, and these

TABLE II. Parameters of the effective-range expansion for electron and positron scattering from argon: $A = -R^*/B_0$ (the scattering length), B_1 (zero-energy contribution for p-wave), B_2 (zero-energy contribution for d wave), R_0 (s-wave effective range), R_1 (p-wave effective range), and R_2 (d-wave effective range). The characteristic distance is $R^* = 2.351a_0$ and the characteristic energy is $E^* = 1.212$ eV.

	A (units of a_0)	B_1	B_2	R_0 (units of a_0)	R_1 (units of a_0)	R_2 (units of a_0)
e^--Ar Ref. [26]	−1.51	−0.44	0.21	−0.38	0.06	0.30
e^--Ar Ref. [11]	−1.50	−0.49	0.27	−0.40	0.10	0.36
e^--Ar Ref. [29]	−1.40	−0.46	0.26	−0.66	0.10	0.27
e^+-Ar Ref. [6]	−5.52	−4.34	–	0.94	4.76	–
e^+-Ar Ref. [36]	−4.11	−3.67	–	−1.47	1.97	–
e^+-Ar Ref. [63]	−4.66	−0.65	–	−0.97	−8.00	–

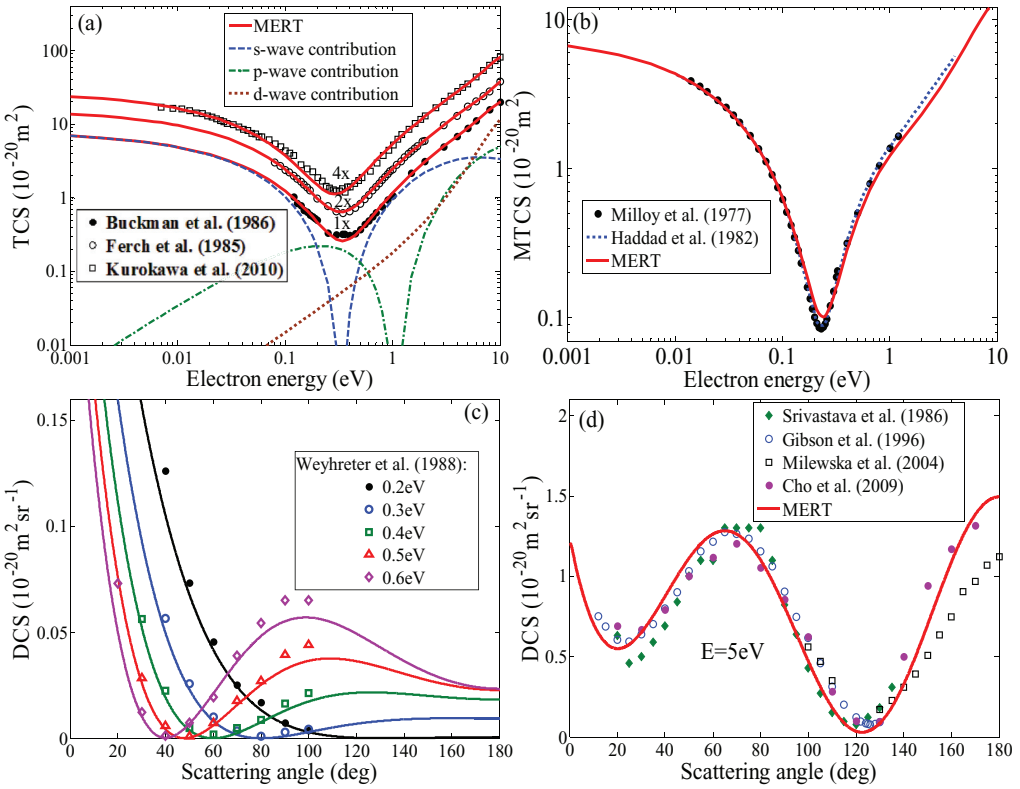

FIG. 3. (Color online) MERT analysis for electron scattering from argon: (a) total cross section versus energy. Experimental data are from [11] (open circles), [26] (filled dots), and [29] (squares). The s- and p-wave contributions are shown only for data of Ref. [26]. (b) Momentum transfer cross section versus energy; swarm-derived data are from [56] (filled dots) and [57] (dotted line). (c) Differential cross section versus scattering angle in the region of R-T minimum compared with data of Weyhreter *et al.* [58]. (d) Differential cross section versus scattering angle at 5 eV; experimental data are from [59] (diamond), [60] (open cricles), [61] (squares), and [62] (filled dots).

values stay in agreement with other published results spanning the range $-2.8a_0$ to $-5.3a_0$ (see [63] and references therein). The existence of the R-T minimum is indicated only by the fit to the data of Karwasz *et al.*, and the derived scattering phase shifts are in good accord with the theoretical results of McEachran *et al.* [64], as shown in Fig. 4(b). The fits to the other two data sets provide only the local minimum of the s-wave phase shifts (not shown here) in the same energy region in such a way that there is no sign change of η_0.

C. Molecular hydrogen

Molecular hydrogen polarizability is $\alpha = 5.314a_0^3$ [44], giving the characteristic range $R^* = 2.305$ eV similar to argon. However, the effective energy $E^* = 2.561$ eV is lower and

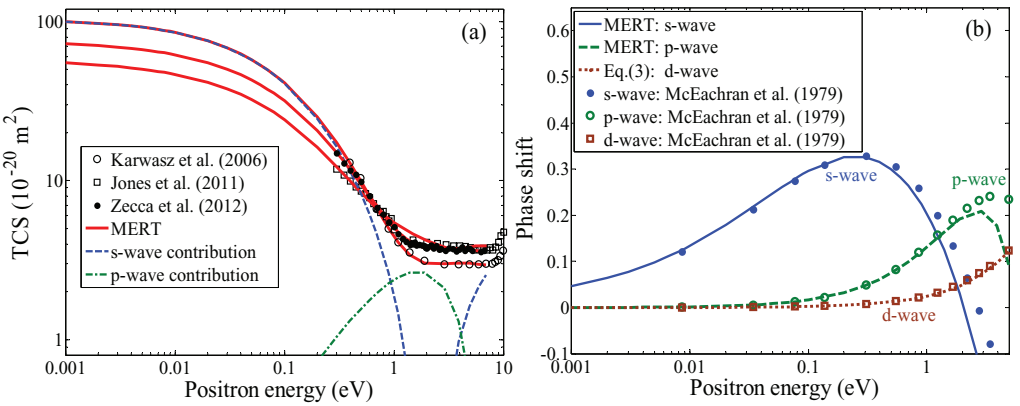

FIG. 4. (Color online) MERT analysis for positron scattering from argon: (a) total cross section versus energy. Experimental data are from Ref. [6] (open circles), [36] (squares), and [63] (filled dots). The s- and p-wave contributions are shown only for data of Ref. [6]. (b) The scattering phase shifts versus energy; solid lines and dashed lines are the MERT calculations for s-wave and p-wave phase shifts based on TCS data of Ref. [6]. Additionally, the dotted line represents the d-wave phase shift estimate by Eq. (3). Present MERT calculations are compared with theoretical results of McEachran *et al.* [64].

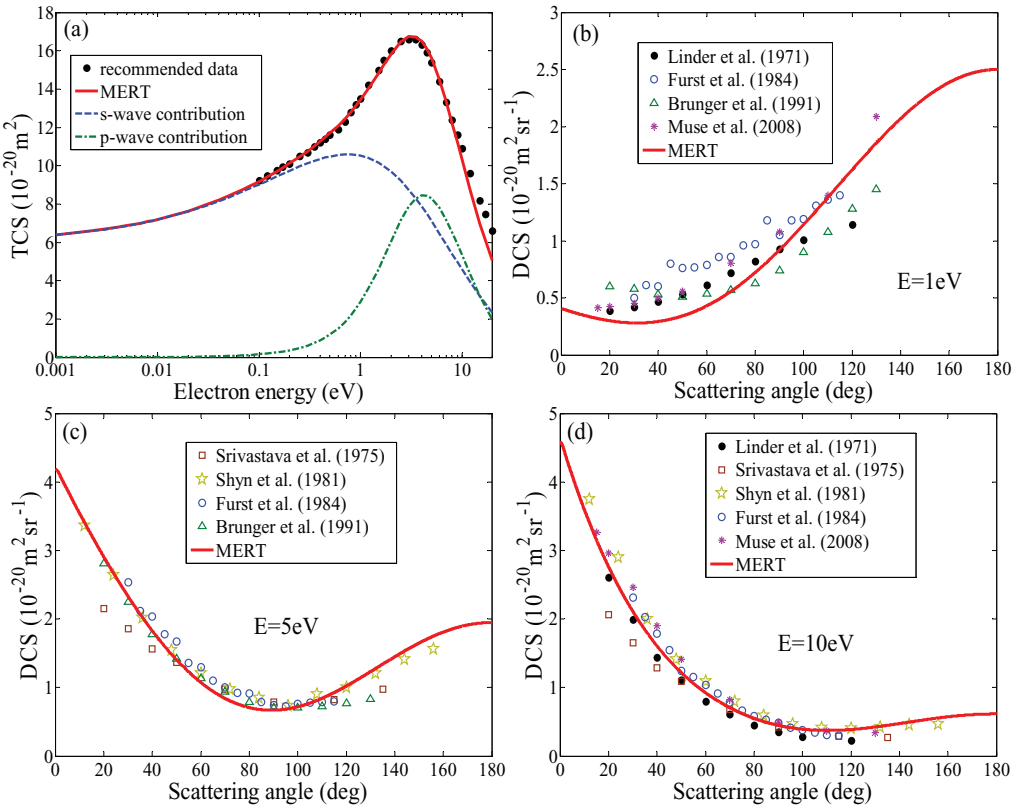

FIG. 5. (Color online) MERT analysis for electron scattering from molecular hydrogen: (a) total cross section versus energy. Dots represent the recommended data from Ref. [66]. (b)–(d) Differential cross section versus scattering angle at 1, 5, and 10 eV, respectively. Experimental data are from [67] (filled dots), [68] (squares), [69] (stars), [70] (open circles), [71] (triangles), and [72] (asterisks).

consequently the corresponding $E_b(2) \approx 23$ eV. As a result the d-wave contribution is expected to be small compared to s and p waves in the energy region $E < 10$ eV where the elastic scattering channel is dominant for both electrons and positrons. Moreover, we assume that the contribution of nonspherical (quadrupole) potential is small in the considered energy range [65]. In Fig. 5(a) we compare the present MERT fit with recommended TCS [66] for electrons. Indeed, the agreement using only two partial waves is very good. The s-wave contribution dominates up to about 1 eV, while at the cross section's maximum (3–4 eV) both the s wave and the p wave give similar contributions. The corresponding parameters of the effective-range expansion are given in Table III. Again the obtained values provide DCS [including the contribution of 100 higher partial waves calculated with Eq. (3)] remaining in very good accord with available experimental data sets [67–72]; see Figs. 5(b)–5(d).

In Fig. 6 we compare the data of Karwasz *et al.* [6] and of Hoffmann *et al.* [73], for positron scattering. The derived MERT parameters are given in Table III. Both sets indicate

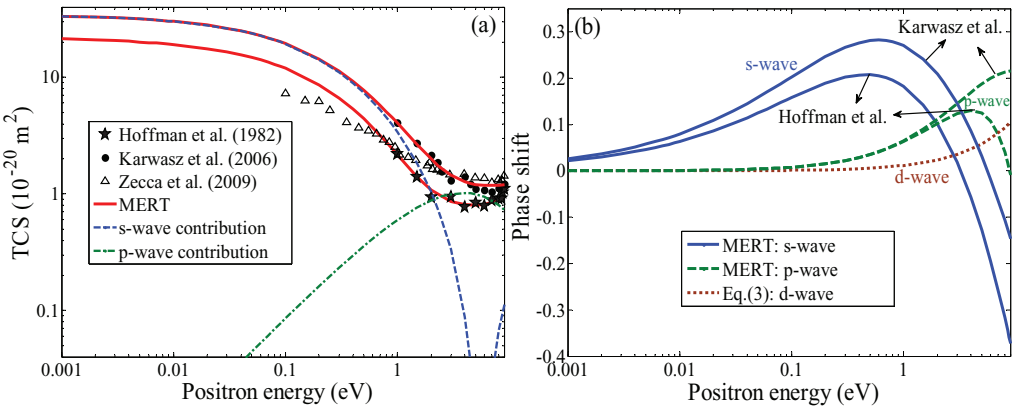

FIG. 6. (Color online) MERT analysis for positron scattering on molecular hydrogen: (a) total cross section versus energy. Experimental data are from Ref. [6] (filled dots), [37] (triangles), and [73] (stars). The s- and p-wave contributions are shown only for data of Ref. [6]. (b) The scattering phase shifts versus the energy. Straight lines are calculations of s-wave phase shifts and dashed lines of p-wave phase shifts using TCS of Refs. [6] and [73]. Additionally, dotted line represents d-wave phase shift estimate by Eq. (3).

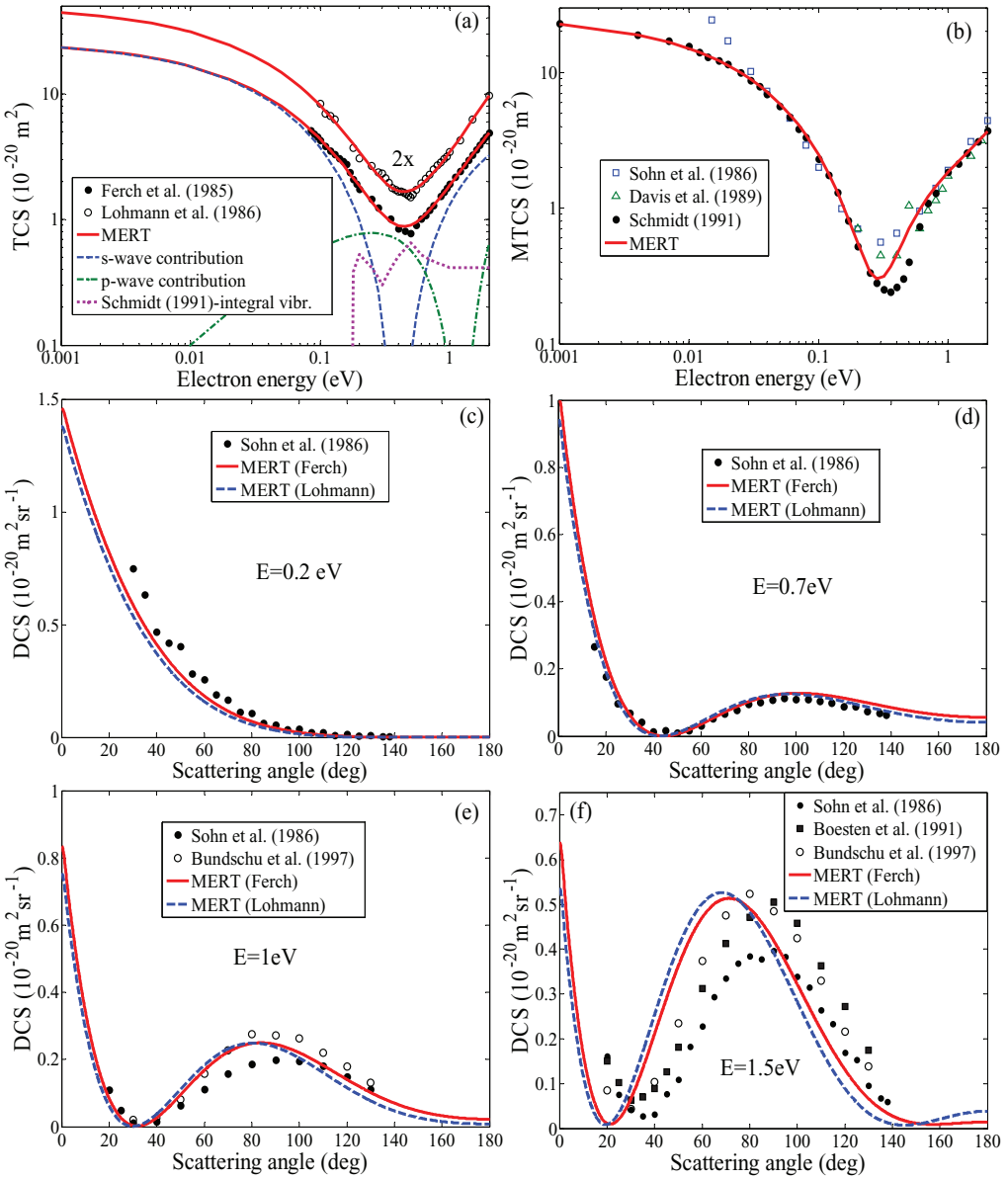

FIG. 7. (Color online) MERT analysis for electron scattering on methane: (a) total cross section versus energy. Experimental data from [10] (filled dots) and [76] (open circles). These data have been subtracted by interpolated vibrational cross sections of Schmidt [31] (dashed line). (b) Momentum transfer cross section versus energy; swarm-derived data are from [31] (filled dots), [77] (squares), and [78] (triangles). (c)–(f). Differential cross section versus the scattering angle at 0.2, 0.7, 1, and 1.5 eV, respectively. Experimental data are from [77] (filled dots), [79] (open circles), and [80] (squares).

TABLE III. Parameters of the effective-range expansion for electron and positron scattering from molecular hydrogen: $A = -R^*/B_0$ (the scattering length), B_1 (zero-energy contribution for p wave), R_0 (s-wave effective range), and R_1 (p-wave effective range). The characteristic distance is $R^* = 2.305a_0$ and the characteristic energy is $E^* = 2.561$ eV.

	A (units of a_0)	B_1	R_0 (units of a_0)	R_1 (units of a_0)
e^--H_2 Ref. [66]	1.30	0.38	−0.92	1.75
e^+-H_2 Ref. [6]	−3.13	−1.99	−0.12	−0.90
e^+-H_2 Ref. [73]	−2.51	−1.94	0.29	−2.51

the existence of an R-T minimum. The scattering length is $-3.13a_0$ for Karwasz *et al.* and smaller at $-2.51a_0$ for the data by Hoffmann *et al.*; this is understandable as the latter data are declared to be underestimated in the low-energy limit due to the weak angular resolution of the Detroit apparatus. Nevertheless, both results are close to the value of $-2.7a_0$ obtained from the *ab initio* calculations of Zhang *et al.* [43]

For comparison purposes we show also in Fig. 6 the more recent data of Zecca *et al.* [37]. However, no reasonable four-parameter MERT fit was possible for this data set. It has been already noted by Zhang *et al.* [43] that the data of Ref. [37] disagree strongly with the theoretical values calculated by the confined variational method [43] and by the Kohn variational method [74], underestimating significantly the scattering

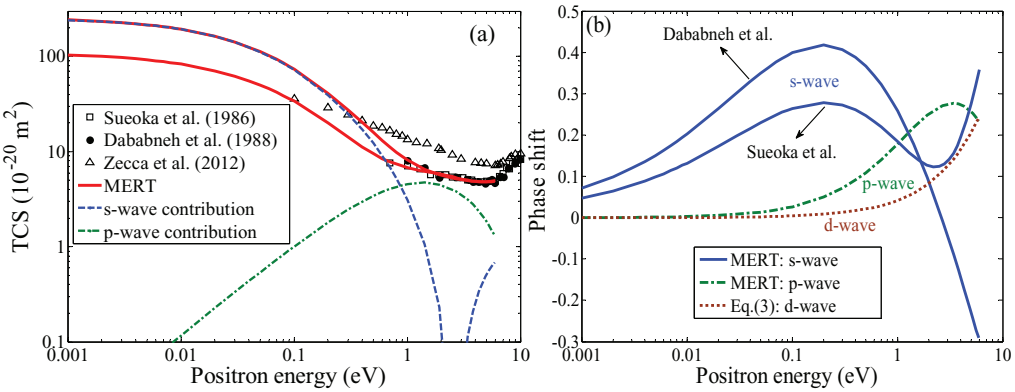

FIG. 8. (Color online) MERT analysis for positron scattering from methane: (a) total cross section versus energy. Experimental data are from Ref. [83] (squares), [84] (filled dots), and [85] (triangles). The s- and p-wave contributions are shown only for data of Ref. [84]. (b) The scattering phase shifts versus the energy. Straight lines are calculations of s-wave phase shifts and dot-dash lines of p-wave phase shifts using TCS of Refs. [83] and [84]. Additionally, the dotted line represents the d-wave phase shift estimate by Eq. (3).

length. In our previous paper [75] we showed that the data by Zecca *et al.* for HCOOH and H_2O measured with the original Trento setup (i.e., with the 10-cm-long scattering cell) can be brought into good agreement with *ab initio* theories if the experimental data are shifted by $+0.2$ eV. It does not seem to be the case for their H_2 data—such a shift brings the scattering length A obtained from the data of Zecca *et al.* [37] to $-2.54a_0$, closer to the value of Zhang *et al.* of $-2.7a_0$, but the "scattering length" for the p wave $1/B_1$ becomes unphysically large.

D. Methane

Knowledge of scattering cross sections for methane (CH_4) is particularly important for tokamak plasma modeling. It has already been shown [10,31] that due to the high symmetry of the molecule the parametrization of scattering phase shifts using MERT is possible for this material. The polarizability of CH_4 is very high, $\alpha = 19.0a_0^3$ [31], and thus the characteristic distance for the polarization interaction is long ($4.36a_0$) and the effective energy is quite low, $E^* = 0.72$ eV. TCS for electron scattering shows a Ramsauer-Townsend minimum at energies similar to those in Ar. However, in order to obtain integral elastic cross sections the vibrational excitation has to be subtracted because it constitutes about 40% of TCS at 0.5 eV. To do this we used vibrational cross sections derived from the drift coefficient by Schmidt [31]. In this work we limit our MERT analysis to energies $E < 2$ eV, where the chosen vibrational excitation cross-section data are available.

We have found that only the two first partial waves are sufficient to reconstruct the experimental TCS of Ferch *et al.* [10] and Lohmann and Buckman [76] in the considered energy range; see Fig. 7(a). The corresponding fitting parameters, given in Table IV, are very similar for both data sets. Consequently, both of them give similar minima in momentum transfer cross sections of about 0.3×10^{-20} m^2 at 0.3 eV; see Fig. 7(b). The current MTCS calculations agree only moderately with the swarm-derived results [31,77,78]; however, swarm experiments are rather old and gas purity is extremely important while measuring drift coefficients in molecular gases. More comparisons will be made in the upcoming work.

We checked also that, with the help of parameters given in Table IV, it is possible to repeat the DCS experimental results quite well [77,79,80] in the whole energy range below 2 eV. Examples of DCS calculations in methane are shown in Figs. 7(c)–7(f). Similarly as for previous targets, MTCS and DCS were obtained using MERT-derived phase shifts, η_0 and η_1, and the contributions of higher partial waves were estimated using Eq. (3). Our DCS results are also in very good agreement with the phase-shift analysis of Sohn *et al.* [77] as well as the *ab initio* calculations of Jain *et al.* [81] and Gianturco *et al.* [82], although the latter work provides lower cross sections at small angles.

For positron scattering (see Fig. 8), two partial waves are sufficient to reproduce the data of the Tokyo [83] and Detroit [84] groups below the positronium formation threshold ($E < 6$ eV). Both data give very similar p-wave phase shifts [in Fig. 8(b) only one dot-dash curve is shown for the sake of clarity]; however, the fit to the Tokyo results provides no Ramsauer-Townsend minimum (no zero at s-wave phase shift). We note that these data were obtained with a relatively high-strength guiding magnetic field and they differ from the Detroit data at the lowest energy measured. Similarly as for molecular hydrogen, we did not manage to approximate the most recent TCS of Zecca *et al.* [85] with any reasonable MERT fit. The positron TCS of Zecca *et al.* were measured on the same version of apparatus as their H_2 data, i.e., using a very short scattering cell.

TABLE IV. Parameters of the effective-range expansion for electron and positron scattering from methane: $A = -R^*/B_0$ (the scattering length), B_1 (zero-energy contribution for p-wave), R_0 (s-wave effective range), and R_1 (p-wave effective range). The characteristic distance is $R^* = 4.36a_0$ and the characteristic energy $E^* = 0.72$ eV.

	A (units of a_0)	B_1	R_0 (units of a_0)	R_1 (units of a_0)
e^--CH_4 Ref. [10]	−2.76	−0.69	−0.34	0.36
e^--CH_4 Ref. [76]	−2.68	−0.84	−0.53	0.50
e^+-CH_4 Ref. [83]	−5.65	−2.82	−1.22	−3.05
e^+-CH_4 Ref. [84]	−8.5	−2.44	−0.25	−4.49

V. CONCLUSIONS

Modified effective-range theory in the analytical form [15] proves to be a powerful tool in analyzing electron and positron cross sections in the low (even up to 10 eV) energy region. Using only a few partial waves within the potential barrier of the target we are able to approximate complex short-range effects and reproduce quite well the integral cross sections. The parameters of the effective-range expansion derived from total elastic cross sections can be used to calculate momentum transfer and differential cross sections, being in very good agreement with available experimental results and some *ab initio* calculations. In this way only four (six) parameters, i.e., the scattering lengths and the effective ranges for the s and p partial waves (sometimes also the d wave), are sufficient to characterize low-energy scattering from atomic and nonpolar molecules (where the small contribution due to the nonspherical nature of the target can be neglected). However, one has to be careful when using MERT since the derived effective-range parameters are very sensitive to the choice of experimental data. Clearly, the k^2 terms in the expansion, representing the effective-range corrections, are relatively small in the low-energy regime in comparison to the leading contribution due to the s-wave scattering length and the p-wave zero-energy contribution. Consequently, the effective-range parameters can be strongly affected by measurement uncertainties in the experimental data in the low-energy domain.

Surprisingly, in positron scattering all four targets, i.e., helium, argon, molecular hydrogen, and methane, show zeros in the s-wave contributions, which should be classified as the existence of Ramsauer-Townsend minima postulated at the dawn of positron experiments by Kauppila and Stein *et al.* [19] These minima are untypical when compared with the Ramsauer-Townsend effect in electron scattering as they occur at relatively high energies and both p and d partial waves bring significant contributions to the cross sections. Characteristically, in the R-T minimum (for both electrons and positrons) the minimum of the s-wave shift is accompanied by the local maximum of the p-wave shift. Thus, the p wave is responsible for the depth of the R-T effect. Nevertheless, these preliminary conclusions should be confirmed by experiments with better energy resolution, much below 10 meV. Experimental data points in lower energies could correct the MERT parameters provided in this paper and thus change energy variations of each partial wave.

ACKNOWLEDGMENT

One of the authors (K. Fedus) would like to acknowledge the support of the Foundation for Polish Science under the START program.

APPENDIX A: STANDARD MERT

Modified effective-range theory (MERT) was proposed by O'Malley *et al.* [8,9] at the beginning of the 1960s. They obtained the low-energy expansions of the scattering phase shifts for electron and positron collisions with atomic and highly symmetric nonpolar molecular targets. These expansions were used to parametrize low-energy collision cross sections using four fitting parameters included in expressions given by Eqs. (1)–(3) [32] and known as the MERT4 version of the original theory. Later higher-order terms in the expansions for p-wave and d-wave phase shifts were introduced by Ali and Fraser [33]. Using these results Buckman and Mitroy [14] proposed a version of the modified effective-range theory with five fitting parameters—MERT5:

$$\tan\eta_0(k) = -Ak\left[1 + \frac{4}{3}\alpha k^2 \ln(k)\right] - \frac{\pi}{3}\alpha k^2 + Dk^3 + Fk^4, \tag{A1}$$

$$\tan\eta_1(k) = a_1\alpha k^2 - A_1 k^3 + (b_1\alpha^2 + c_1\alpha_q)k^4 + Hk^5, \tag{A2}$$

$$\tan\eta_l(k) = a_l\alpha k^2 + (b_l\alpha^2 + c_l\alpha_q)k^4 \quad \text{for } l \geqslant 2, \tag{A3}$$

where A is the scattering length and D, F, A_1, and H are additional parameters. Here α_q is the difference of two components, the static quadrupole polarizability and the nonadiabatic dipole polarizability, which is calculated from the nonadiabatic correction. Generally α_q is very small because these two components are opposite in sign and are of almost the same magnitude. Coefficients a_l, b_l, and c_l are given by

$$a_l = \frac{\pi}{(2l+1)(2l-1)(2l+3)}, \tag{A4}$$

$$b_l = \frac{\pi[15(2l+1)^4 - 140(2l+1)^2 + 128]}{[(2l+1)(2l-1)(2l+3)]^3 (2l+5)(2l-3)}, \tag{A5}$$

$$c_l = \frac{3a_l}{(2l+5)(2l-3)}. \tag{A6}$$

Moreover, since MERT5 was not sufficient to describe the d-wave phase shift for some noble gases in a satisfactory way, Buckman and Mitroy proposed also an MERT6 version by adding the sixth fitting parameter, A_2, in the formula with $l = 2$ [14]:

$$\tan\eta_2(k) = a_2\alpha k^2 + (b_2\alpha^2 + c_2\alpha_q)k^4 + A_2 k^5. \tag{A7}$$

Another extension of standard MERT was proposed by O'Malley and Crompton [24] in order to enlarge the valid energy region for representation of the s-wave phase shift. It was done by adding the seventh parameter, G, in Eq. (A1):

$$\tan\eta_0(k) = \frac{-Ak\left[1 + \frac{4}{3}\alpha k^2 \ln(k)\right] - \frac{\pi}{3}\alpha k^2 + Dk^3 + Fk^4}{1 + Gk^3}, \tag{A8}$$

Equation (A8) becomes identical to Eq. (A1) at $k \to 0$.

APPENDIX B: ANALYTICAL APPROACH TO MERT

The long-range polarization interaction of a charged particle (electron, positron) with an atom (or a neutral molecule) is described by the following Schrödinger equation in the relative coordinate [8]:

$$\left[\frac{\partial^2}{\partial r^2} - \frac{l(l+1)}{r^2} + \frac{\beta}{r^4} + k^2\right]\Psi_l(r) = 0, \tag{B1}$$

where $\beta = \alpha e^2\mu/\hbar^2$. The effective potential is composed of a centrifugal barrier $l(l+1)r^{-2}$ and a long-range ($r \to \infty$) dipole polarization term βr^{-4}. To solve Eq. (B1) we substitute $r = \sqrt{R^*}e^{-z}/\sqrt{k}$ and $\Psi_l(r) = \psi(r)\sqrt{r/R^*}$, which yields

Mathieu's modified differential equation [8]:

$$\frac{\partial^2\psi}{\partial z^2} - [a - 2q\cosh 2z]\,\psi = 0, \tag{B2}$$

where $a = (l + 1/2)^2$ and $q = kR^*$. Two linearly independent solutions, $M_v(z)$ and $T_v(z)$, can be expressed in the following form:

$$M_v(z) = \sum_{n=-\infty}^{\infty} (-1)^n c_n(v) J_{2n+v}(2\sqrt{q}\cosh z), \tag{B3}$$

$$T_v(z) = \sum_{n=-\infty}^{\infty} (-1)^n c_n(v) Y_{2n+v}(2\sqrt{q}\cosh z), \tag{B4}$$

where v is the characteristic exponent, and $J_v(z)$ and $Y_v(z)$ are Bessel and Neumann functions, respectively.

The characteristic exponent appearing in Eq. (7) for the scattering phase shift can be calculated numerically from

$$\cos\pi v = 1 - \Delta(1 - \cos\pi\sqrt{a}), \tag{B5}$$

where Δ is an infinite determinant (independent of v):

$$\Delta = \begin{vmatrix} \ddots & \vdots & \vdots & \vdots & \vdots & \vdots & \\ \cdots & 1 & \gamma_{-2} & 0 & 0 & 0 & \cdots \\ \cdots & \gamma_{-1} & 1 & \gamma_{-1} & 0 & 0 & \cdots \\ \cdots & 0 & \gamma_0 & 1 & \gamma_0 & 0 & \cdots \\ \cdots & 0 & 0 & \gamma_1 & 1 & \gamma_1 & \cdots \\ \cdots & 0 & 0 & 0 & \gamma_2 & 1 & \cdots \\ & \vdots & \vdots & \vdots & \vdots & \vdots & \ddots \end{vmatrix}, \tag{B6}$$

where $\gamma_n = q/(4n^2 - a)$. Typically, determinant Δ converges very fast, and it is sufficient to take relatively small matrices to calculate it [34].

To determine the remaining unknown parameter m in Eq. (7) it is necessary to exploit the asymptotic properties of $M_v(z)$, $T_v(z)$, and $W_v(z)$, as described in detail in Refs. [15,16,34]. Here $W_v(z)$ is a different representation for the solutions of Mathieu's equation:

$$W_v(z) = \sum_{n=-\infty}^{\infty} c_n(v)\, e^{(2n+v)z}, \tag{B7}$$

where c_n are the same coefficients as used in Eqs. (B3) and (B4). The parameter m is defined as

$$m = \kappa \lim_{z\to 0^+} W_v(z)/W_{-v}(z), \tag{B8}$$

where $\kappa = M_v(z)\,W_{-v}(z)/M_{-v}(z)\,W_v(z)$ is a constant prefactor determined for some moderate values of the argument $z \approx 1$. To find unknown c_n coefficients in the wave functions we substitute the ansatz (B3) and (B4) into Eq. (B2) in order to obtain the recurrence relation

$$[(2n + v)^2 - a]c_n + q(c_{n-1} + c_{n+1}) = 0, \tag{B9}$$

which can be solved in terms of continued fractions. To do this we introduce $h_n^+ = c_n/c_{n-1}$ and $h_n^- = c_{-n}/c_{-n+1}$ for $n > 0$, which, when substituted into Eq. (B9), gives the continued fractions

$$h_n^+ = -\frac{q}{qh_{n+1}^+ + d_n} \quad \text{and} \quad h_n^- = -\frac{q}{qh_{n+1}^- + d_{-n}}, \tag{B10}$$

where $d_n = (2n + v)^2 - a$. In practice, to find numerical values of the coefficients c_n, we set $h_{n'}^+ = 0$ and $h_{n'}^- = 0$ for some sufficiently large n' and calculate h_n^+ and h_n^- up to $n = 1$. Then $c_n = h_n^+ h_{n-1}^+ \cdots h_1^+ c_0$ and $c_{-n} = h_n^- h_{n-1}^- \cdots h_1^- c_0$, where, for the purpose of the calculations, it is convenient to assume $c_0 = 1$.

[1] W. M. Huo and Y. K. Kim, IEEE Trans. Plasma Sci. **27**, 1225 (1999).
[2] J.-S. Yoon, Y.-W. Kim, D.-C. Kwon, M.-Y. Song, W.-S. Chang, C.-G. Kim, V. Kumar, and B. Lee, Rep. Prog. Phys. **73**, 116401 (2010).
[3] J. Tennyson, Phys. Rep. **491**, 29 (2010).
[4] G. P. Karwasz, Eur. Phys. J. D **35**, 267 (2005).
[5] C. M. Surko, G. F. Gribakin, and S. J. Buckman, J. Phys. B **38**, R57 (2005).
[6] G. P. Karwasz, D. Pliszka, and R. S. Brusa, Nucl. Instrum. Methods Phys. Res., Sect. B **247**, 68 (2006).
[7] W. Tenfen, K. T. Mazon, S. E. Michelin, J. R. Mohallem, and D. Assafrao, J. Phys.: Conf. Ser. **388**, 052021 (2012).
[8] T. F. O'Malley, L. Spruch, and L. Rosenberg, J. Math. Phys. **2**, 491 (1961).
[9] T. F. O'Malley, L. Rosenberg, and L. Spruch, Phys. Rev. **125**, 1300 (1962).
[10] J. Ferch, B. Granitza, and W. Raith, J. Phys. B **18**, L445 (1985).
[11] J. Ferch, B. Granitza, and W. Raith, J. Phys. B **18**, 967 (1985).
[12] A. Mann and F. Linder, J. Phys. B **25**, 533 (1992).
[13] G. P. Karwasz, A. Karbowski, Z. Idziaszek, and R. S. Brusa, Nucl. Instrum. Methods Phys. Res., Sect. B **266**, 471 (2008).
[14] S. J. Buckman and J. Mitroy, J. Phys. B **22**, 1365 (1989).
[15] Z. Idziaszek and G. Karwasz, Phys. Rev. A **73**, 064701 (2006).
[16] Z. Idziaszek and G. Karwasz, Eur. Phys. J. D **51**, 347 (2009).
[17] A. Zecca, G. P. Karwasz, and R. S. Brusa, Riv. Nuovo Cim. **19**(3), 30 (1996).
[18] G. P. Karwasz, A. Zecca, and R. S. Brusa, Riv. Nuovo Cim. **24**(1), 12 (2001).
[19] T. S. Stein, W. E. Kauppila, V. Pol, J. H. Smart, and G. Jesion, Phys. Rev. A **17**, 1600 (1978).
[20] J. M. Blatt and J. D. Jackson, Phys. Rev. **76**, 18 (1949).
[21] H. A. Bethe, Phys. Rev. **76**, 38 (1949).
[22] T. F. O'Malley, Phys. Rev. **130**, 1020 (1963).
[23] D. E. Golden, Phys. Rev. **151**, 48 (1966).
[24] T. F. O'Malley and R. W. Crompton, J. Phys. B **13**, 3451 (1980).
[25] G. N. Haddad and T. F. O'Malley, Aust. J. Phys. **35**, 35 (1982).
[26] S. J. Buckman and B. Lohmann, J. Phys. B: At. Mol. Phys. **19**, 2547 (1986).
[27] M. Weyhreter, B. Barzick, A. Mann, and F. Linder, Z. Phys. D **7**, 333 (1987).
[28] J. P. England and M. T. Elford, Aust. J. Phys. **41**, 701 (1988).
[29] M. Kurokawa, M. Kitajima, K. Toyoshima, T. Kishino, T. Odagiri, H. Kato, M. Hoshino, H. Tanaka, and K. Ito, Phys. Rev. A **84**, 062717 (2011).

[30] M. Kitajima, M. Kurokawa, T. Kishino, K. Toyoshima, T. Odagiri, H. Kato, K. Anzai, M. Hoshino, H. Tanaka, and K. Ito, Eur. Phys. J. D **66**, 130 (2012).
[31] B. Schmidt, J. Phys. B **24**, 4809 (1991).
[32] T. F. O'Malley, Phys. Rev. **130**, 120 (1963).
[33] M. K. Ali and P. A. Fraser, J. Phys. B **10**, 3091 (1977).
[34] Z. Idziaszek, A. Simoni, T. Calarco, and P. S. Julienne, New J. Phys. **13**, 083005 (2011).
[35] G. P. Karwasz, D. Pliszka, A. Zecca, and R. S. Brusa, Nucl. Instrum. Methods Phys. Res., Sect. B **240**, 666 (2005).
[36] A. C. L. Jones, C. Makochekanwa, P. Caradonna, D. S. Slaughter, J. R. Machachek, R. P. McEachran, J. P. Sullivan, S. J. Buckman, A. D. Stauffer, I. Bray, and D. V. Fursa, Phys. Rev. A **83**, 032701 (2011).
[37] A. Zecca, L. Chiari, A. Sarkar, K. L. Nixon, and M. J. Brunger, Phys. Rev. A **80**, 032702 (2009).
[38] J. P. Sullivan, C. Makochekanwa, A. Jones, P. Caradonna, D. S. Slaughter, J. Machacek, R. P. McEachran, D. W. Mueller, and S. J. Buckman, J. Phys. B **44**, 035201 (2011).
[39] O. Sueoka and S. Mori, J. Phys. Soc. Jpn. **53**, 2491 (1984).
[40] G. P. Karwasz, D. Pliszka, A. Zecca, and R. S. Brusa, J. Phys. B **38**, 1 (2005).
[41] G. Karwasz, R. S. Brusa, M. Barozzi, and A. Zecca, Nucl. Instrum. Methods Phys. Res., Sect. B **171**, 178 (2000).
[42] A. Zecca, L. Chiari, A. Sarkar, K. L. Nixon, and M. J. Brunger, Phys. Rev. A **80**, 032702 (2009).
[43] J.-Y. Zhang, J. Mitroy, and K. Varga, Phys. Rev. Lett. **103**, 223202 (2009).
[44] T. N. Olney, N. M. Cann, G. Cooper, and C. E. Brion, Chem. Phys. **223**, 59 (1997).
[45] PHELPS database, http://www.lxcat.laplace.univ-tlse.fr; R. W. Crompton, M. T. Elford, and R. L. Jory, Aust. J. Phys. **20**, 369 (1967); R. W. Crompton, M. T. Elford, and A. G. Robertson, *ibid.* **23**, 667 (1970); H. B. Milloy and R. W. Crompton, Phys. Rev. A **15**, 1847 (1977) at low energy, and M. Hayashi, Institute of Plasma Physics Report No. IPPJ-AM-19, 1981, at high energies.
[46] D. Andrick and A. Bitsch, J. Phys. B **8**, 393 (1975).
[47] D. F. Register, S. Trajmar, and S. K. Srivastava, Phys. Rev. A **21**, 1134 (1980).
[48] T. W. Shyn, Phys. Rev. A **22**, 916 (1980).
[49] M. J. Brunger, S. J. Buckman, L. J. Allen, I. E. McCarthy, and K. Ratnavelu, J. Phys. B **25**, 1823 (1992).
[50] T. S. Stein, W. E. Kauppila, V. Pol, J. H. Smart, and G. Jesion, Phys. Rev. A **17**, 1600 (1978).
[51] T. Mizogawa, Y. Nakayama, T. Kawaratani, and M. Tosaki, Phys. Rev. A **31**, 2171 (1985).
[52] J. P. Sullivan, C. Makochekanwa, A. Jones, P. Caradonna, and S. Buckman, J. Phys. B **41**, 081001 (2008).
[53] R. P. McEachran, D. L. Morgan, A. G. Ryman, and A. D. Stauffer, J. Phys. B **10**, 663 (1977).
[54] J. Y. Zhang and J. Mitroy, Phys. Rev. A **78**, 012703 (2008).
[55] P. Van Reeth and J. W. Humberston, J. Phys. B **32**, 3651 (1999).
[56] H. B. Milloy, R. W. Maeda, J. A. Rees, and A. G. Robertson, Aust. J. Phys. **30**, 61 (1977).
[57] G. N. Haddad and T. F. O'Malley, Aust. J. Phys. **35**, 35 (1982).
[58] M. Weyhreter, B. Barzick, A. Mann, and F. Linder, Z. Phys. D **7**, 333 (1988).
[59] S. K. Srivastava, H. Tanaka, A. Chutjian, and S. Trajmar, Phys. Rev. A **23**, 2156 (1981).
[60] J. C. Gibson, R. J. Gulley, J. P. Sullivan, S. J. Buckman, V. Chan, and P. D. Burrow, J. Phys. B **29**, 3177 (1996).
[61] B. Mielewska, I. Linert, G. C. King, and M. Zubek, Phys. Rev. A **69**, 062716 (2004).
[62] H. Cho and Y. S. Park, J. Korean Phys. Soc. **55**, 459 (2009).
[63] A. Zecca, L. Chiari, E. Trainotti, D. V. Fursa, I. Bray, A. Sarkar, S. Chattopadhyay, K. Ratnavelu, and M. J. Brunger, J. Phys. B **45**, 015203 (2012).
[64] R. P. McEachran, A. G. Ryman, and A. D. Stauffer, J. Phys. B **12**, 1031 (1979).
[65] S. Hara, J. Phys. Soc. Jpn. **22**, 710 (1967).
[66] G. P. Karwasz, A. Zecca, and R. S. Brusa, in *Photon and Electron Interactions with Atoms, Molecules and Ions*, Landolt-Börnstein New Series, Vol. I/17 (Springer-Verlag, Berlin, Heidelberg, 2003), pp. 6.1–6.51.
[67] F. Linder and H. Schmidt, Z. Naturforsch. A **26**, 1603 (1971).
[68] S. K. Srivastava, A. Chutjian, and S. Trajmar, J. Chem. Phys. **63**, 2659 (1975).
[69] T. W. Shyn and W. E. Sharp, Phys. Rev. A **24**, 1734 (1981).
[70] J. Furst, M. Mahgerefteh, and D. E. Golden, Phys. Rev. A **30**, 2256 (1984).
[71] M. J. Brunger, S. J. Buckman, D. S. Newman, and D. T. Alle, J. Phys. B **24**, 1435 (1991).
[72] J. Muse, H. Silva, M. C. A. Lopes, and M. A. Khakoo, J. Phys. B **41**, 095203 (2008).
[73] K. R. Hoffman, M. S. Dababneh, Y.-F. Hsieh, W. E. Kauppila, V. Pol, J. H. Smart, and T. S. Stein, Phys. Rev. A **25**, 1393 (1982).
[74] E. A. G. Armour and D. J. Baker, J. Phys. B **19**, L871 (1986).
[75] G. P. Karwasz, R. S. Brusa, and D. Pliszka, J. Phys.: Conf. Ser. **199**, 012019 (2010).
[76] B. Lohmann and S. J. Buckman, J. Phys. B **19**, 2565 (1986).
[77] W. Sohn, K. H. Kochem, K. M. Scheuerlein, K. Jung, and H. Ehrhardt, J. Phys. B **19**, 3625 (1986).
[78] D. K. Davies, L. E. Kline, and W. E. Bies, J. Appl. Phys. **65**, 3311 (1989).
[79] C. T. Bundschu, J. C. Gibson, R. J. Gulley, M. J. Brunger, S. J. Buckman, N. Sanna, and F. A. Gianturco, J. Phys. B **30**, 2239 (1997).
[80] L. Boesten and H. Tanaka, J. Phys. B **24**, 821 (1991).
[81] A. Jain, C. A. Weatherford, D. G. Thompson, and P. McNaughten, Phys. Rev. A **40**, 6730 (1989).
[82] F. A. Gianturco, J. A. Rodriguez-Ruiz, and N. Sanna, J. Phys. B **28**, 1287 (1995).
[83] O. Sueoka and S. Mori, J. Phys. B **19**, 4035 (1986).
[84] M. S. Dababneh, Y.-F. Hsieh, W. E. Kauppila, C. K. Kwan, Steven J. Smith, T. S. Stein, and M. N. Uddin, Phys. Rev. A **38**, 1207 (1988).
[85] A. Zecca, L. Chiari, E. Trainotti, A. Sarkar, S. d'A. Sanchez, M. H. F. Bettega, M. T. do N. Varella, M. A. P. Lima, and M. J. Brunger, Phys. Rev. A **85**, 012707 (2012).